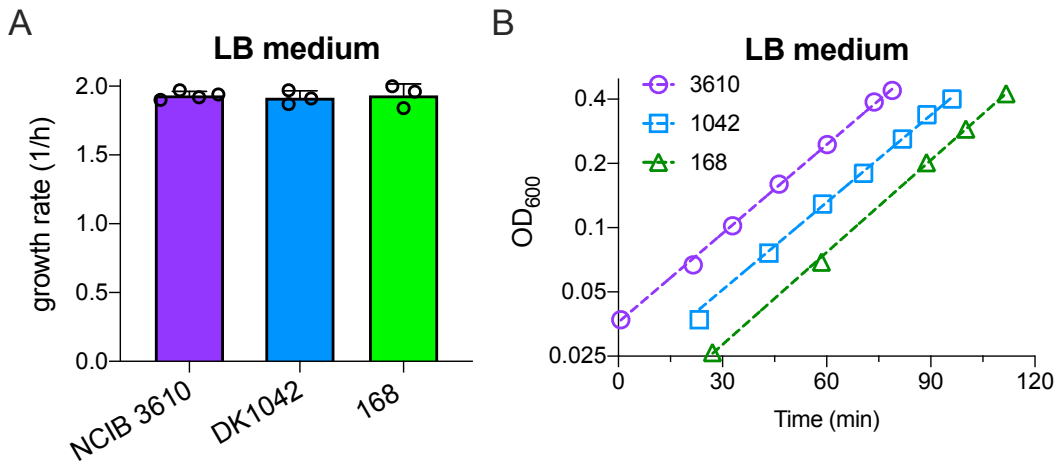

Figure S1. The exponential growth rates (panel A) and typical growth curves (panel B) of NCIB 3610 strain, DK1042 strain and 168 strain in LB nutrient broth. Data are presented as the mean values +/- standard deviations (SD) of several biological replicates (n=4, 3, 3 for NCIB3610, DK1042 and 168, respectively). Source data are provided as a Source Data file.

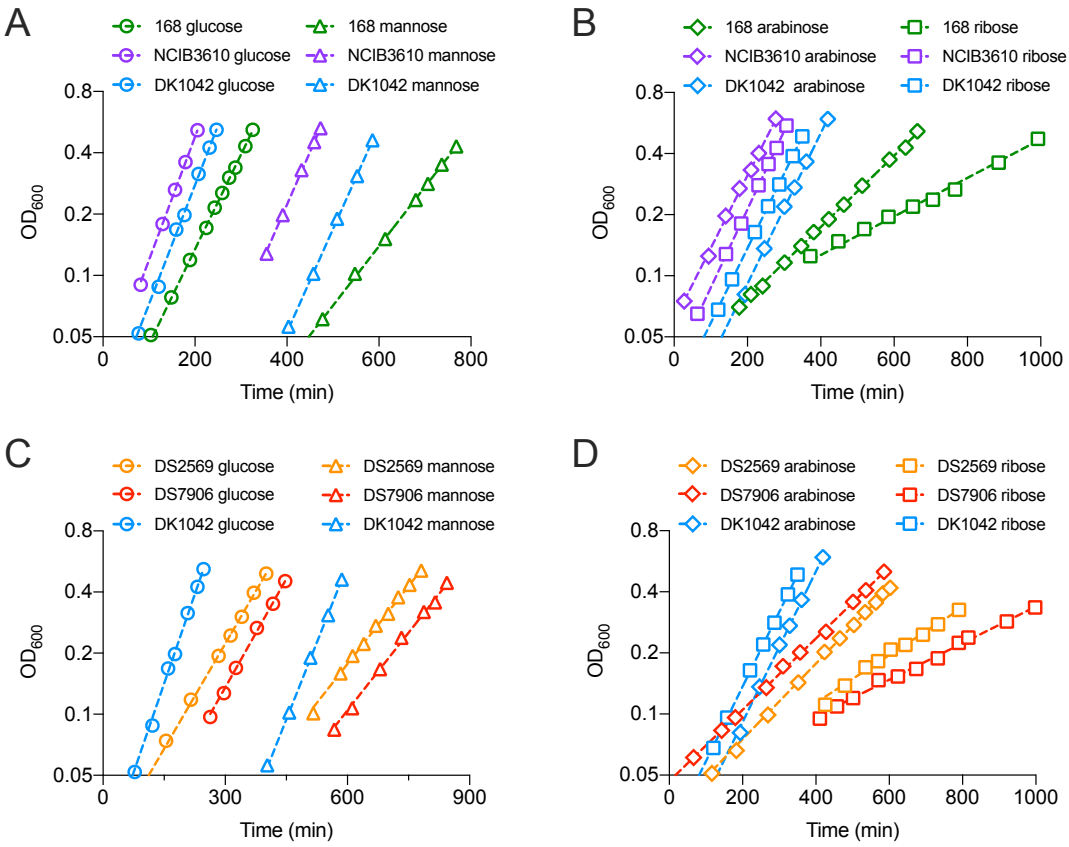

Figure S2. Typical exponential growth curves of undomesticated and domesticated *B. subtilis* strains on various carbon sources. These strains include the domesticated 168 strain, the NCIB 3610 ancestral strain, the DK1042 strain (the *comI*^{Q12L} 3610 strain) (panel A and B), the pBS32-cured DS2569 strain and the *rapP*-null DS7906 strain (panel C and D). Source data are provided as a Source Data file.

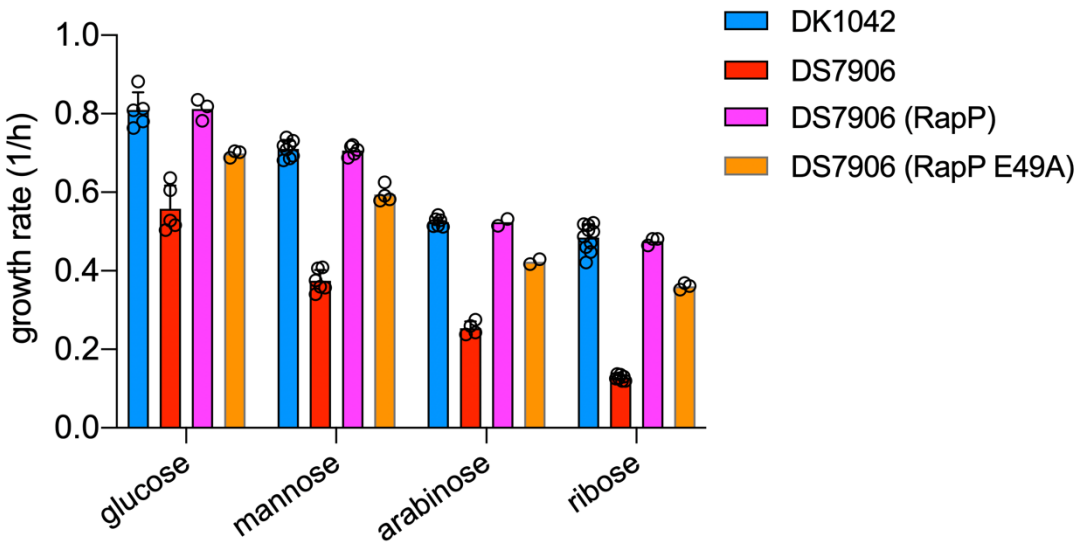

Figure S3. The effect of complementation of RapP and its E49A mutant (phosphatase inactive form) on the growth rates of DS7906 on various carbon sources. The native *PrapP-rapP* cassette in pBS32 as well as the *rapP* (E49A) mutant version was inserted into pHT01 plasmid and further transformed to DS7906 strain. Data are presented as the mean values +/- standard deviations (SD) of several biological replicates. For DK1042 strain: n=5, 8, 6, 10 for glucose, mannose, arabinose and ribose, respectively. For DS7906 strain: n=5, 6, 4, 7 for glucose, mannose, arabinose and ribose, respectively. For DS7906 (RapP) strain: n=3, 5, 2, 3 for glucose, mannose, arabinose and ribose, respectively. For DS7906 (RapP E49A) strain: n=3, 4, 2, 3 for glucose, mannose, arabinose and ribose, respectively. Source data are provided as a Source Data file.

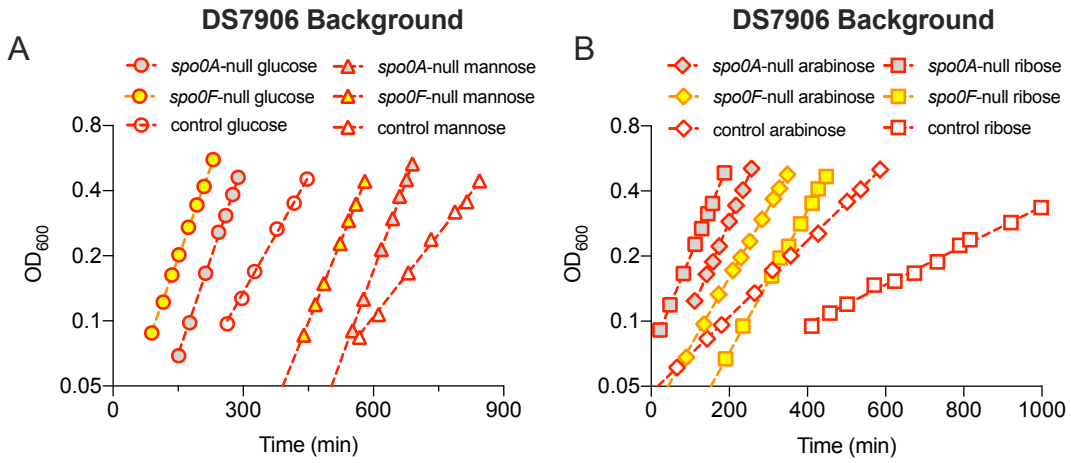

Figure S4. Typical exponential growth curves of *B. subtilis* DS7906 strain and its *spo0F-null, spo0A-null* strains on various carbon sources including glucose, mannose shown in panel A and arabinose, ribose shown in panel B. Control refers to the original DS7906 strain. Source data are provided as a Source Data file.

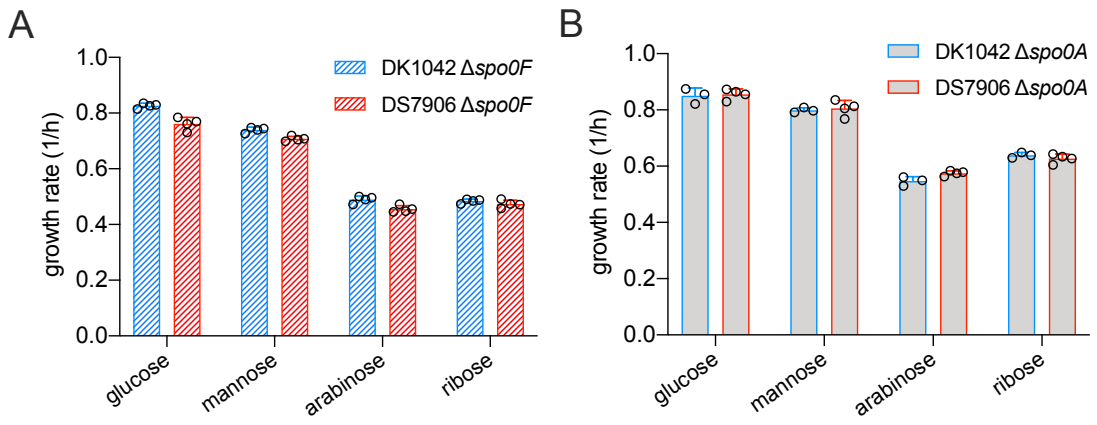

Figure S5. (A) Growth rates of DK1042 *spo0F*-null strain and DS7906 *spo0F*-null strain. **(B)** Growth rates of DK1042 *spo0A*-null strain and DS7906 *spo0A*-null strain. Data are presented as the mean values +/- standard deviations (SD) of several biological replicates. n=4 for all the conditions in panel A. n=3 and 4 for DK1042 and DS7906 strains, respectively, in panel B. Source data are provided as a Source Data file.

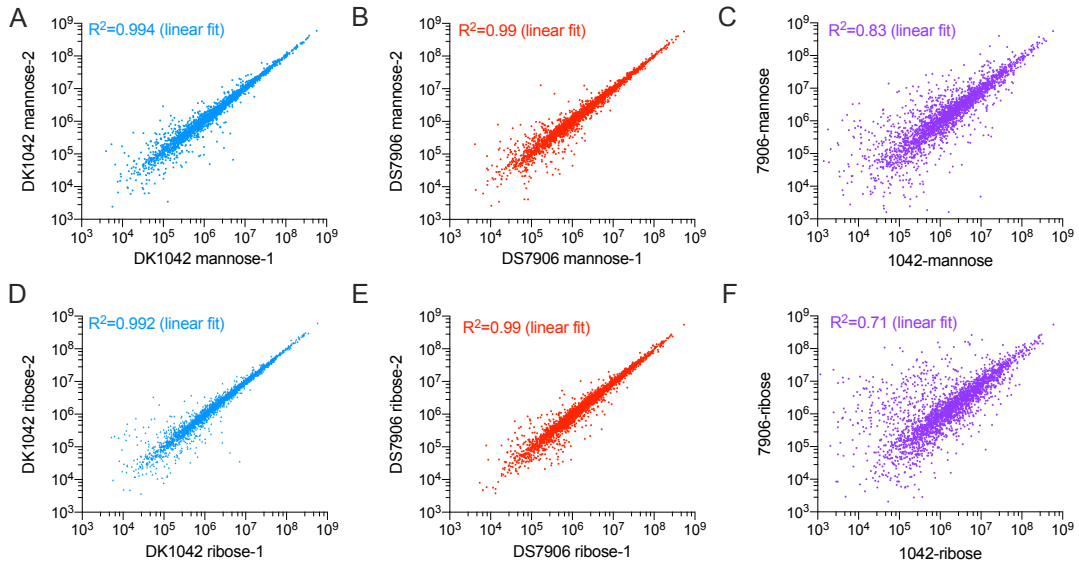

Figure S6. Scatter plots of the "iBAQ mass" of individual proteins between pairs of replicates or conditions in XA1826LQ project. There are four conditions studied in XA1826LQ project including two strains on two carbon sources: DK1042 strain and DS7906 strain growing on mannose and ribose, respectively (supplementary data 2). Each condition contains two replicates. We used "iBAQ mass" (Mol Weight × iBAQ intensity) as a proxy of the mass abundance of each protein as iBAQ was a proxy of the copy number of protein. From panel A, B, D and E, we found that the linear correlation between data of the two replicates of each condition was high (R^2=0.99), suggesting high reproducibility. In contrast, the linear correlations between the data of DS7906 strain and DK1042 strain was lower (panel C and F), suggesting large amounts of differentially expressed genes in the two strains. Source data of IBAQ mass are provided in supplementary data 2.

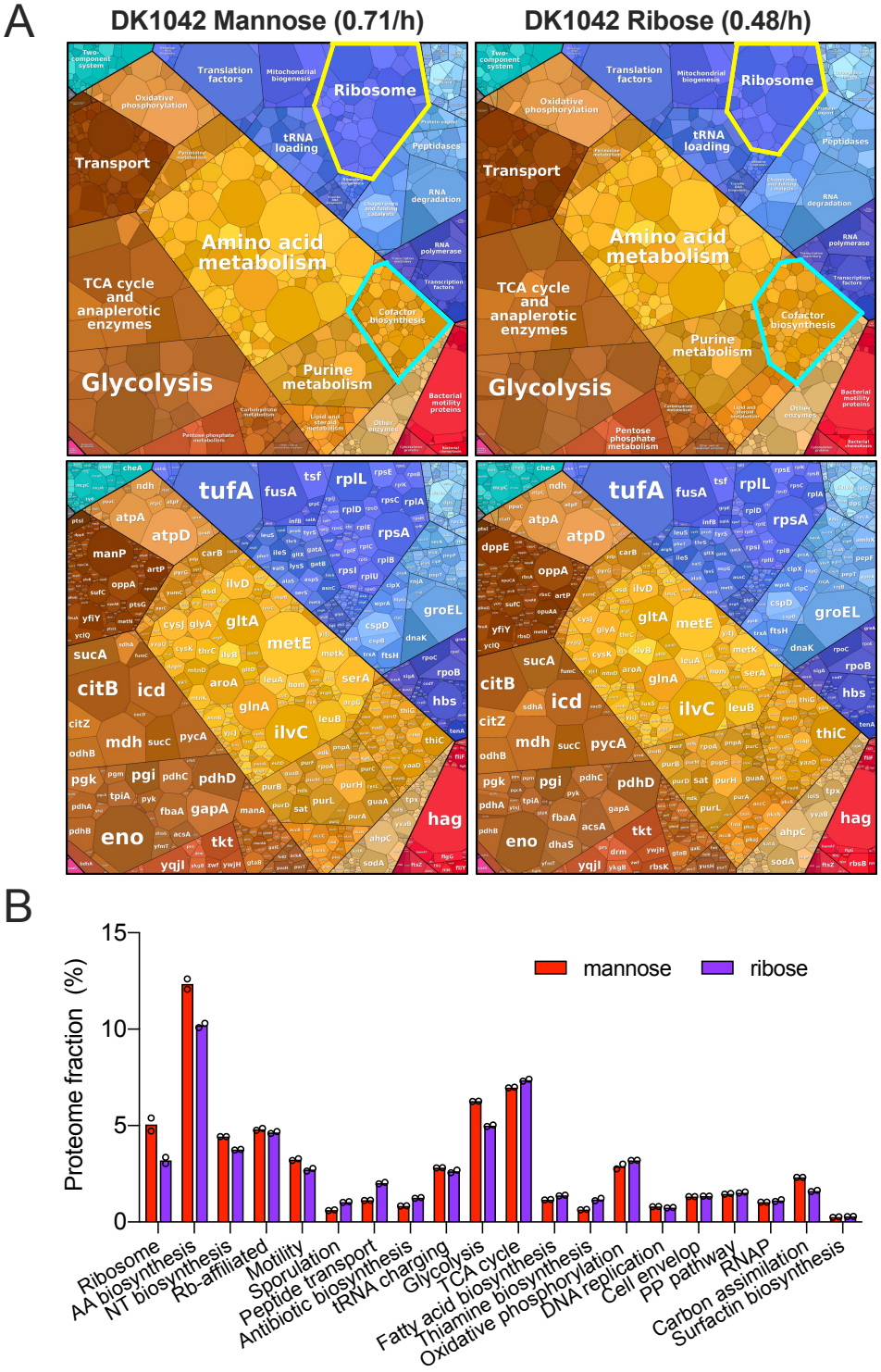

Figure S7. Proteome allocations of DK1042 strain growing in mannose and ribose media. **(A)** Proteome allocation of DK1042 strain in mannose and ribose media visualized by the proteomaps website. **(B)** The mass fractions of various functional proteome sectors of DK1042 strain. Individual data points correspond to two biological replicates (n=2). Source data are provided as a Source Data file.

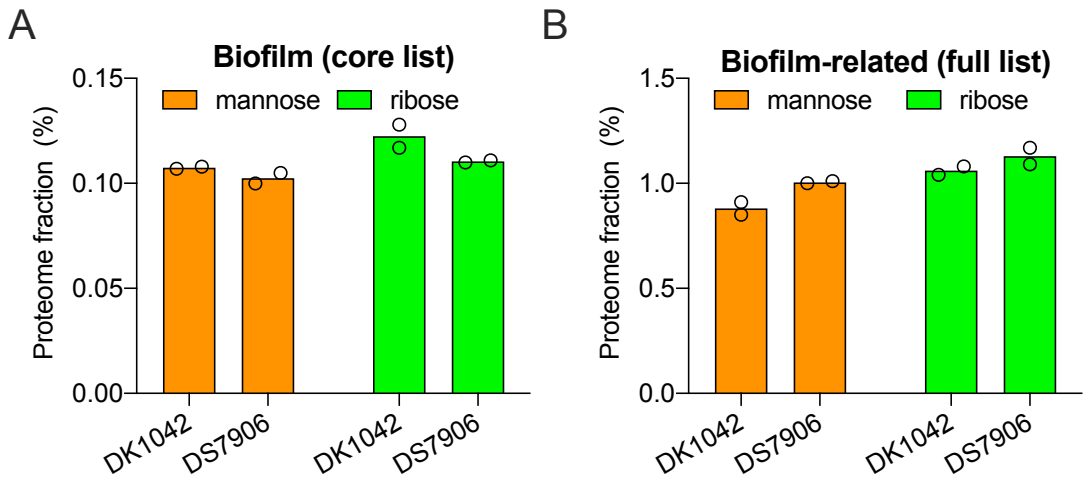

Figure S8. The proteome fractions of biofilm-related proteins in DK1042 and DS7906 strains. (A) The proteome fractions of structural proteins that directly involved in biofilm formation such as matrix polysaccharide synthesis, amyloid protein synthesis, secretion and assembly. This list is referred to as core list of biofilm-related proteins. **(B)** The proteome fractions of a full list of biofilm-related proteins that includes not only structural proteins but also proteins regulate the biofilm formation. Individual data points correspond to two biological replicates (n=2). Source data are provided as a Source Data file.

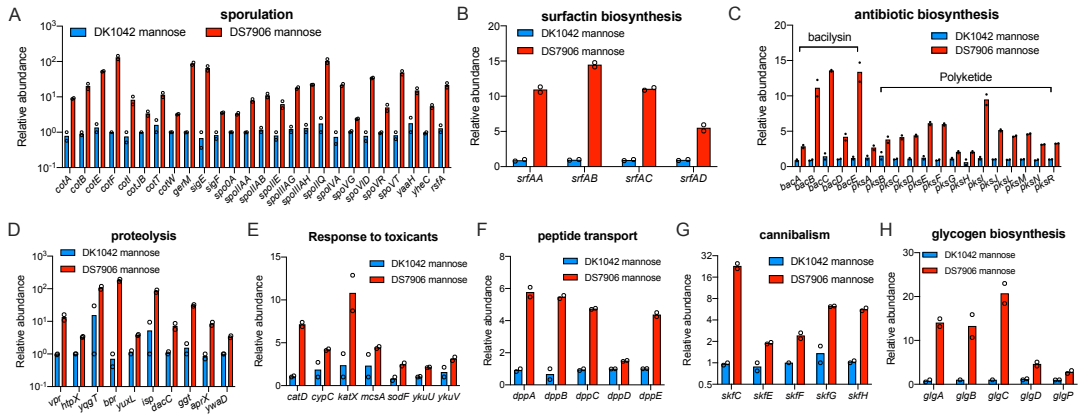

Figure S9. Various adaptive response pathways that are induced in *rapP*-null DS7906 strain compared with *rapP*$^{+}$ DK1042 strain, including sporulation (panel A), surfactin biosynthesis (panel B), antibiotic biosynthesis (panel C), proteolysis (Panel D), response to toxicants (pane E), peptide transport (panel F), cannibalism (panel G) and glycogen biosynthesis (panel H). The abundance refers to the proteome mass fraction of each protein (using the data of iBAQ mass). Individual data points correspond to two biological replicates (n=2). Source data are provided as a Source Data file.

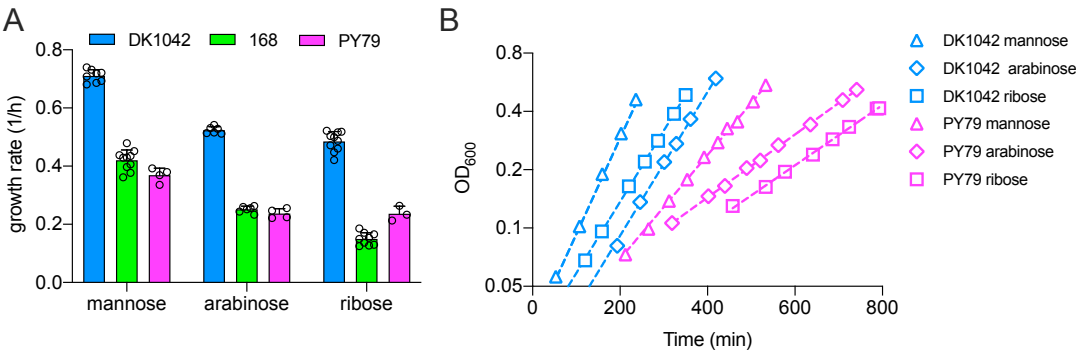

Figure S10. The growth rates (panel A) and typical growth curves (panel B) of DK1042, 168 and PY79 strains on various carbon sources. Data are presented as the mean values +/- standard deviations (SD) of several biological replicates (for PY79 strain: n=4, 4, 3 for mannose, arabinose and ribose, respectively; for DK1042 strain: n=8, 6, 10 for mannose, arabinose and ribose, respectively; for 168 strain: n=10, 6, 9 for mannose, arabinose and ribose, respectively). Source data are provided as a Source Data file.

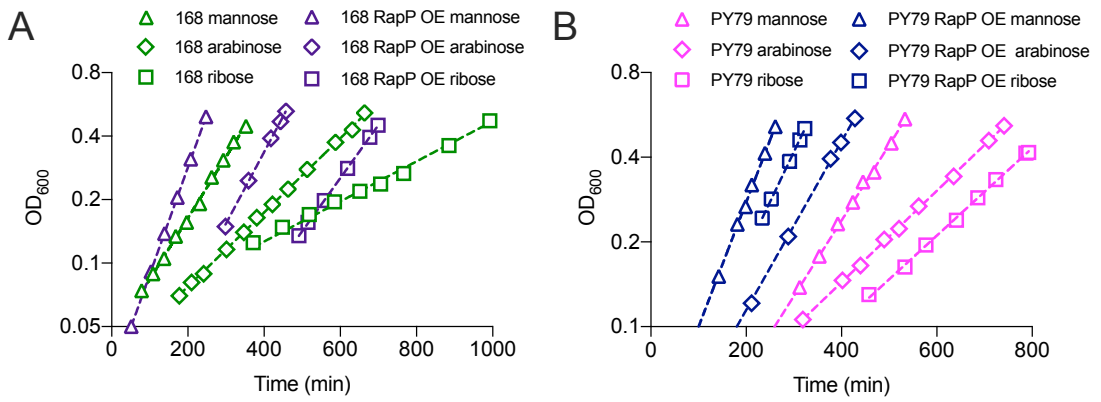

Figure S11. The growth rates of 168 (panel A) and PY79 strains (panel B) upon RapP overexpression (OE) on various carbon sources. 400 μM IPTG was added to the medium of RapP OE strain (for PY79 strain growing in mannose medium, 300 μM IPTG was added). Source data are provided as a Source Data file.

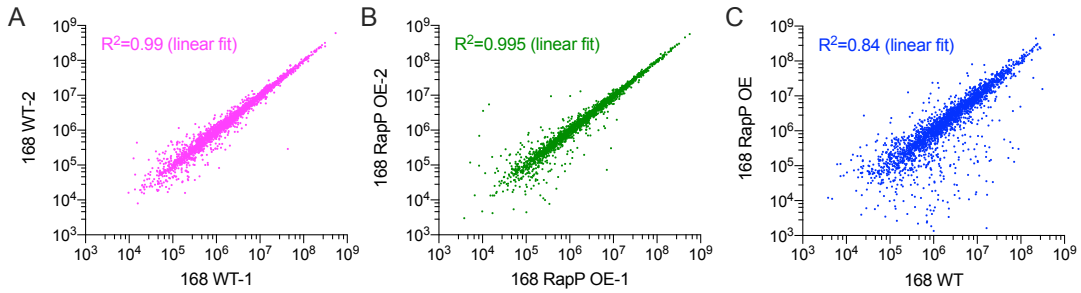

Figure S12. Scatter plots of the "iBAQ mass" of individual proteins between pairs of replicates or conditions in XA1827LQ project. XA1827LQ project contains two conditions, the wild type 168 and its RapP-overexpressing strain in ribose medium (supplementary data 5-7). 400 μM IPTG was added to the medium of RapP-overexpressing strain. Each condition contains two replicates. We used iBAQ mass (Mol Weight × iBAQ intensity) as a proxy of the mass abundance of each protein as iBAQ was a proxy of the copy number of protein. From panel A and B, we found that the linear correlation between the data of the two replicates of each condition was high (R^2=0.99), suggesting high reproducibility. In contrast, the linear correlation between the data of wild type 168 and its RapP-overexpressing strains was lower (panel C), again suggesting large amounts of differentially expressed genes in the two strains. Source data of IBAQ mass are provided in supplementary data 6.

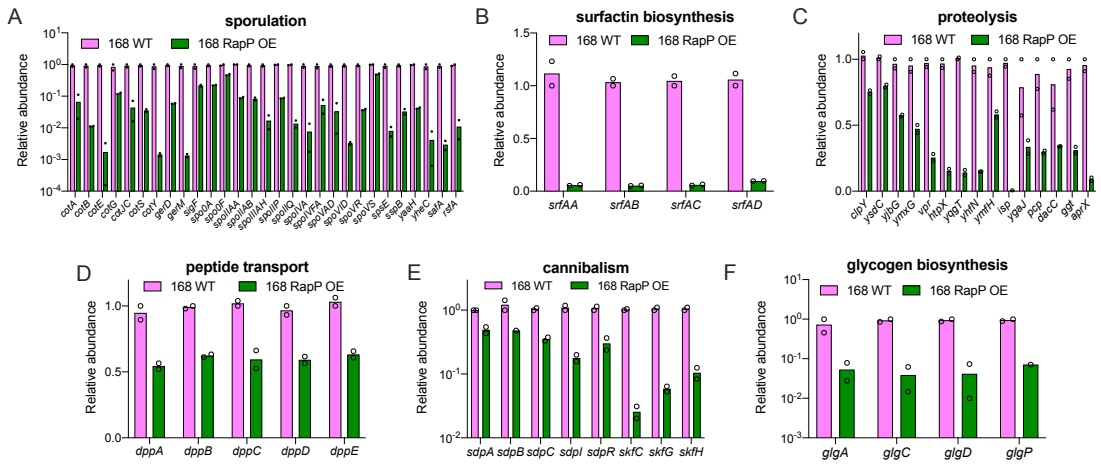

Figure S13. Various adaptive response pathways that are downregulated upon RapP overexpression (OE) in 168 strain, including sporulation (panel A), surfactin biosynthesis (panel B), proteolysis (panel C), peptide transport (panel D), cannibalism (panel E) and glycogen biosynthesis (panel F). The abundance refers to the proteome mass fraction of each protein (using the data of iBAQ mass). Individual data points correspond to two biological replicates (n=2). Source data are provided as a Source Data file.